7

COHERENT TRAIN OF LFM PULSES

Good Doppler resolution requires a long coherent signal. To minimize eclipsing requires a short transmission time (unless the radar is especially designed to transmit and receive simultaneously, as in CW radar). A solution that meets both requirements is a coherent train of pulses. The basic type of such a signal was discussed in Sections 3.6 and 4.3, where the train was constructed from identical constant-frequency pulses. In many practical cases the pulses are modulated and are not identical. Modulation produces wider bandwidth, hence pulse compression. The identicalness is violated by even the simple introduction of interpulse weighting, used to lower Doppler sidelobes. In some signals, significant diversity is introduced between the pulses in order to obtain additional advantages, such as lower delay sidelobes or lower recurrent lobes.

In this and the following chapters we extend the discussion in two directions: adding modulation and adding diversity. Adding modulation but keeping the pulses identical still allows us to use the theoretical results regarding the periodic ambiguity function (Section 3.6) and to obtain analytic expression for the ambiguity function (within the duration of one pulse, i.e., $|\tau| \leq T$). Adding diversity in amplitude (i.e., weighting) or by different modulation in different pulses within the coherent train will usually require numerical analysis, except for a few simple cases in which theoretical analysis is available. Such is the case for the subject of this chapter—a coherent train of LFM pulses—probably the most popular radar signal in airborne radar (Rihaczek, 1969; Stimson, 1983; Nathanson et al., 1991).

Radar Signals, By Nadav Levanon and Eli Mozeson
ISBN 0-471-47378-2

7.1 COHERENT TRAIN OF IDENTICAL LFM PULSES

A train of identical linear-FM pulses provides both range resolution and Doppler resolution—hence its importance and popularity in radar systems. Its ambiguity function still suffers from significant sidelobes, both in delay (range) and in Doppler. Thus, modifications are usually applied to reduce these sidelobes. In this section we consider the basic signal without modifications. The coherency is reflected in the expression of the real signal, given by

$$s(t) = \mathrm{Re}[u(t)\exp(j2\pi f_c t)] \tag{7.1}$$

where the complex envelope is a train of N pulses with pulse repetition period T_r,

$$u(t) = \frac{1}{\sqrt{N}}\sum_{n=1}^{N} u_n[t-(n-1)T_r] \tag{7.2}$$

The uniformity of the pulses is expressed by assuming that $u_n(t) = u_1(t)$. The LFM nature of a pulse of duration T is expressed in its complex envelope,

$$u_1(t) = \frac{1}{\sqrt{T}}\mathrm{rect}\left(\frac{t}{T}\right)\exp(j\pi kt^2), \qquad k = \pm\frac{B}{T} \tag{7.3}$$

An example of a real signal is shown in Fig. 7.1, where all the pulses begin with the same initial phase. This is not a mandatory requirement for coherence. Coherency can be maintained as long as the initial phase of each pulse transmitted is known to the receiver.

Changes in phase from pulse to pulse will be expressed in the complex envelope of the nth pulse as

$$u_n(t) = \frac{1}{\sqrt{T}}\mathrm{rect}\left(\frac{t}{T}\right)\exp[j(\phi_n + \pi kt^2)], \qquad k = \pm\frac{B}{T} \tag{7.4}$$

As long as $T < T_r/2$ (which will be assumed henceforth), the additional phase element has no effect on the ambiguity function for $|\tau| \le T$. It will only affect the recurrent lobes of the AF: namely, over $|\tau \pm nT_r| \le T$ $(n = 1, 2, \ldots)$. The

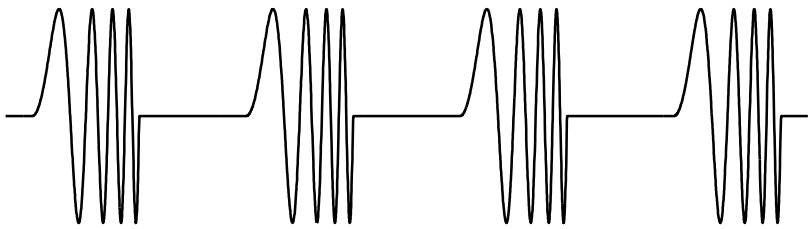

FIGURE 7.1 Coherent train of identical LFM pulses.

additional phase term can already be considered as some sort of diversity, but one that affects only recurrent lobes.

To get an analytic expression for the partial ambiguity function (AF) of our signal, we start with the AF of a constant-frequency pulse, apply AF property 4 to it, and obtain the AF of a single LFM pulse (as done in Section 4.2):

$$|\chi(\tau, \nu)| = |\chi_T(\tau, \nu)| = \left| \left(1 - \frac{|\tau|}{T}\right) \frac{\sin \alpha}{\alpha} \right|, \qquad |\tau| \le T \quad \text{(single pulse)} \tag{7.5}$$

where

$$\alpha = \pi T \left(\nu \mp B\frac{\tau}{T}\right)\left(1 - \frac{|\tau|}{T}\right) \tag{7.6}$$

The first equality $|\chi(\tau, \nu)| = |\chi_T(\tau, \nu)|$ stems from the fact that $T < T_r/2$. To describe the AF of the train, for the limited delay $|\tau| \le T$, we now apply the relationship of the periodic AF:

$$|\chi(\tau, \nu)| = |\chi_T(\tau, \nu)| \left| \frac{\sin N\pi\nu T_r}{N \sin \pi\nu T_r} \right|, \qquad |\tau| \le T \quad \text{(train of pulses)} \tag{7.7}$$

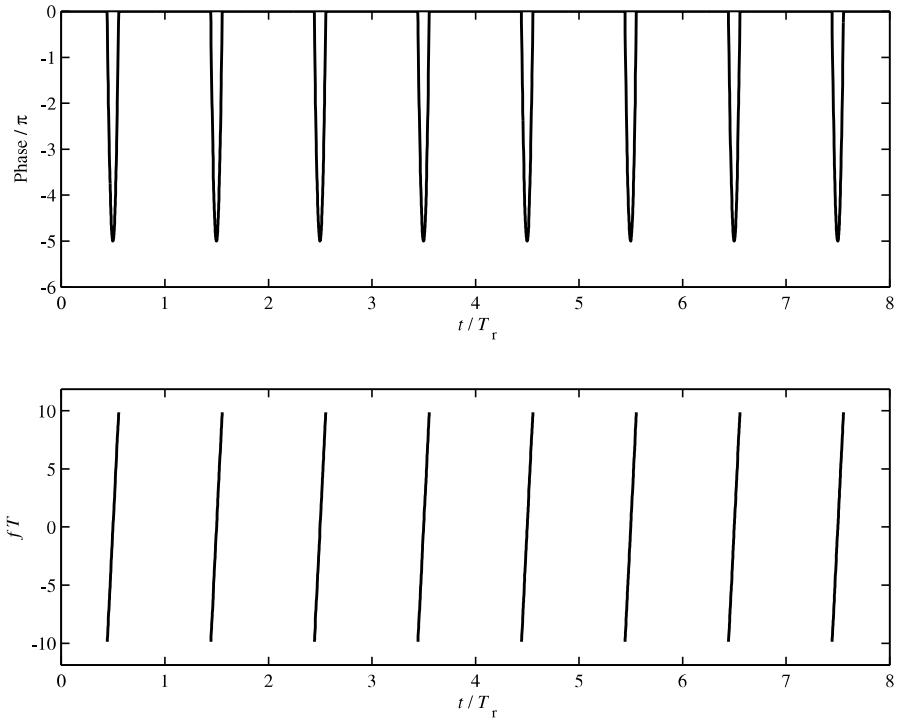

FIGURE 7.2 Phase (top) and frequency (bottom) of a coherent train of eight LFM pulses ($BT = 20$).

Using (7.5) in (7.7) yields the ambiguity function of a train of N identical LFM pulses:

$$|\chi(\tau, \nu)| = \left|\left(1 - \frac{|\tau|}{T}\right)\frac{\sin\alpha}{\alpha}\right|\left|\frac{\sin N\pi\nu T_r}{N\sin\pi\nu T_r}\right|, \qquad |\tau| \le T \tag{7.8}$$

We will demonstrate the signal and its AF using a train of eight LFM pulses. The time–bandwidth product of each pulse is 20 and the duty cycle is $T/T_r = \frac{1}{9}$. The phase and frequency history are given in Fig. 7.2. The partial ambiguity function, plotted in Fig. 7.3, is restricted in delay to ± 1 pulse width, and in Doppler to $10/8 = 1.25$ the pulse repetition frequency (PRF, $1/T_r$). Note the first null in Doppler that occurs at $\nu = 1/(NT_r) = 1/(8T_r) = 1/T_c$, where $T_c = 8T_r$ is the coherent processing time. This improved Doppler resolution is the main contribution of the pulse train. Note also the first recurrent Doppler peak at $\nu = 1/T_r$. It is difficult to note from the plot, but the recurrent Doppler lobe is slightly lower and slightly delayed compared to the main lobe. The zero-Doppler cut of Fig. 7.3 (i.e., the magnitude of the normalized autocorrelation function) is identical to the cut that would have been obtained with a single LFM pulse. This is a property of all trains of *identical* pulses. An AF plot extending beyond the first delay recurrent lobe is plotted in Fig. 7.4, and an AF plot extending over the

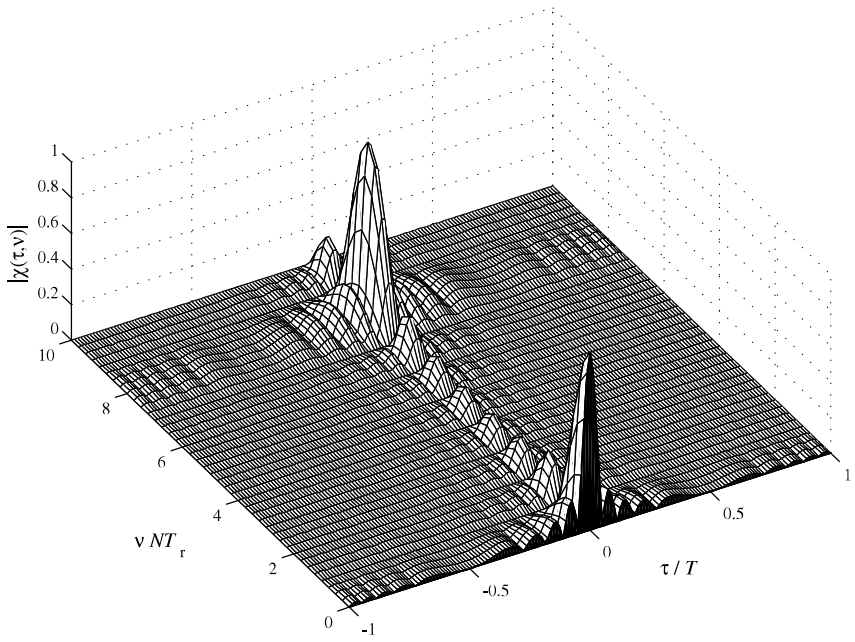

FIGURE 7.3 Partial ambiguity function ($|\tau| \le T$) of a coherent train of eight LFM pulses ($BT = 20$).

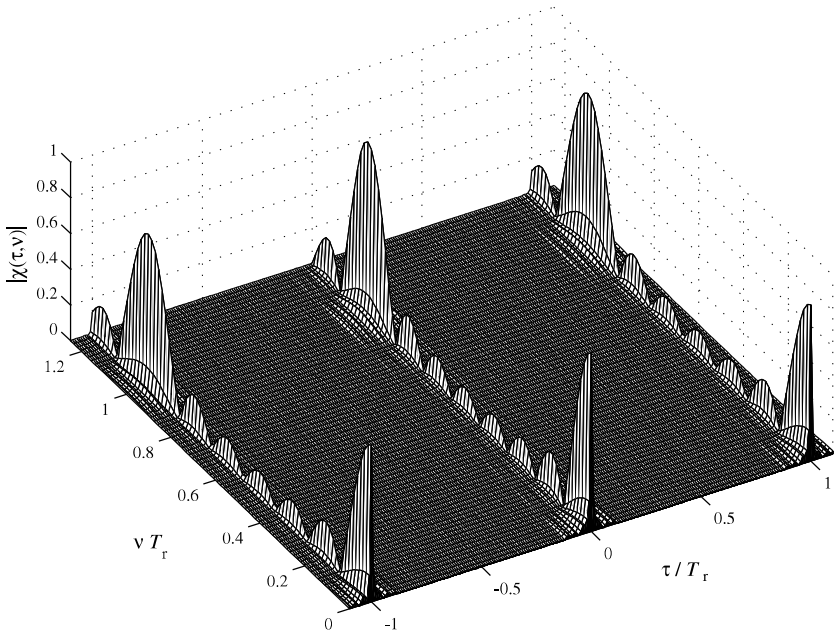

FIGURE 7.4 Partial ambiguity function ($|\tau| \leq T + T_r$) of a coherent train of eight LFM pulses ($BT = 20$).

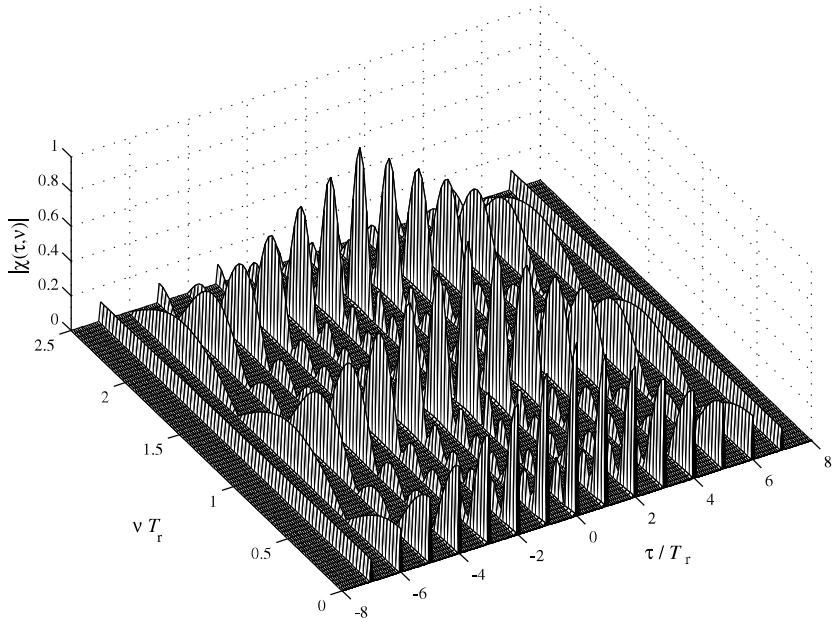

FIGURE 7.5 Ambiguity function ($|\tau| \leq 8T_r$) of a coherent train of eight LFM pulses ($BT = 20$).

entire delay span appears in Fig. 7.5. The Doppler span displayed was doubled in Fig. 7.5, showing two Doppler recurrent lobes.

7.2 FILTERS MATCHED TO HIGHER DOPPLER SHIFTS

The ambiguity function displays the response of a filter matched to the original signal, without Doppler shift. As shown in Fig. 7.3, a coherent pulse train achieves good Doppler resolution, and a matched filter will produce an output only when the Doppler shift of the received signal is within the Doppler resolution. A typical radar processor is likely to contain several filters, matched to several different Doppler shifts. In a coherent pulse train, implementing such a processor is relatively simple, especially if the intrapulse modulation is Doppler tolerant, as LFM is.

The principle of Doppler filter implementation is summarized in Figs. 7.6 and 7.7. Figure 7.6 shows that each pulse is processed by a zero-Doppler matched filter. The N outputs from the N pulses are then fed to an FFT. The first output of the FFT is equivalent to a zero-Doppler filter. For that first output the FFT coherently sums the N inputs. For the second FFT output, the nth pulse $n = 0, 1, \ldots, N-1$ is first multiplied by the complex coefficient $\exp(j2\pi n/N)$, before being added to the outputs of the other N processed pulses. This complex coefficient is equivalent to a phase shift,

$$\phi_n = 2\pi\frac{n}{N} = 2\pi\nu n T_r \Rightarrow \nu = \frac{1}{NT_r} \tag{7.9}$$

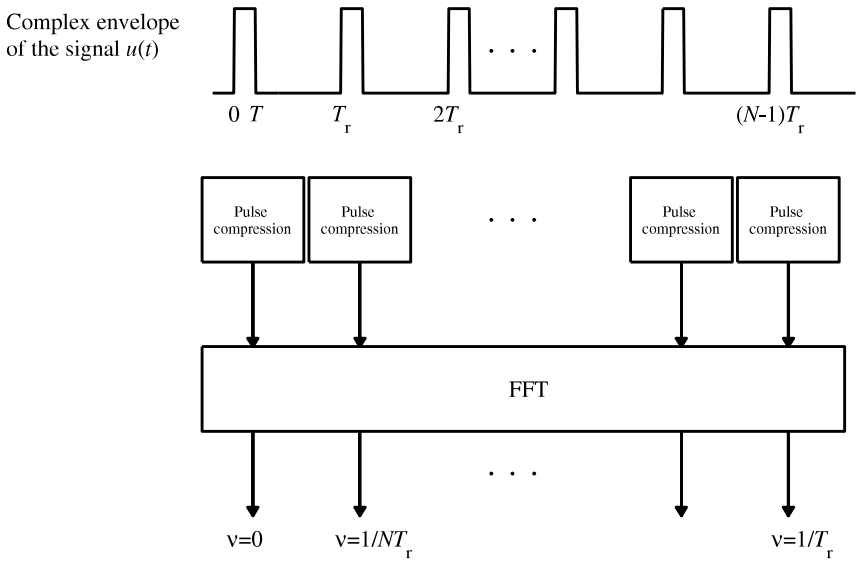

FIGURE 7.6 Implementing several Doppler filters using FFT.

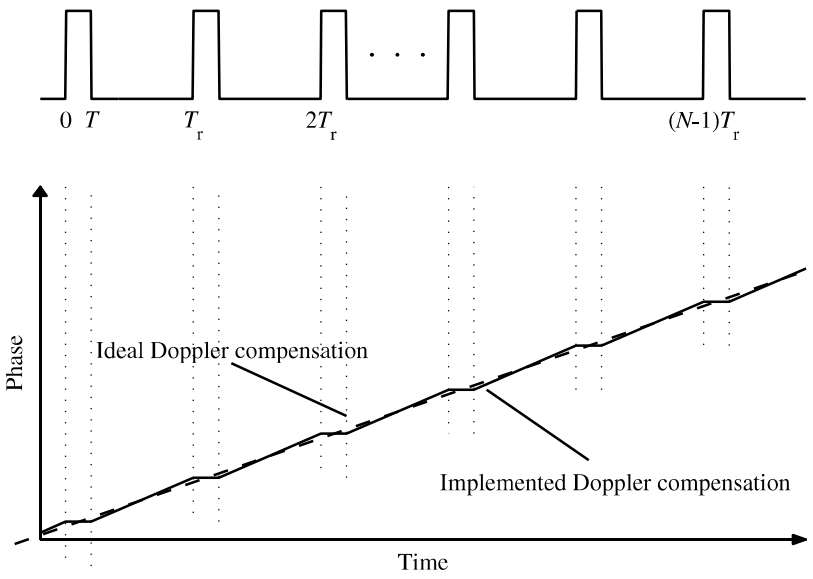

FIGURE 7.7 Interpulse phase compensation for a higher Doppler filter.

The phase shift ϕ_n, added to the nth pulse which is delayed by nT_r, is equal to the phase shift that would have been accumulated after a delay of nT_r by a Doppler shift of $v = 1/NT_r$. We thus see that the second output of the FFT is effectively a Doppler filter matched to the Doppler frequency at which the first Doppler filter produces a null response. (The first Doppler filter is centered at zero Doppler.) The $(k + 1)$ FFT filter sums the pulses after multiplying the nth pulse by the complex coefficient $\exp(j2\pi kn/N)$, and is therefore matched to a Doppler frequency $v = k/NT_r$ or because of Doppler ambiguity (mod $1/T_r$), to $v = -(N - k)/NT_r$.

The Doppler compensation achieved by this method is represented by the solid line in Fig. 7.7. The ideal Doppler compensation is represented by the dashed line. The difference is that the FFT implementation lacks Doppler compensation within each pulse. If the output of a compressed pulse is relatively insensitive to Doppler shift (like LFM), the performance of the FFT approach is nearly as good as the performance of an ideal Doppler filter.

The expected response of the second Doppler filter (matched to $v = 1/NT_r$) of the train of eight LFM pulses studied in Section 7.1 is shown in Fig. 7.8. The response was obtained by calculating a cross-ambiguity function between two signals, one having the normal phase history of a train of identical LFM pulses (Fig. 7.9, top), and the other in which phase steps of $2\pi/N = \pi/4$ were added between pulses (Fig. 7.9, bottom). Note in Fig. 7.8 that the response was zero at zero Doppler and peaked at $v = 1/NT_r$, while in Fig. 7.3 the response peaks at zero Doppler and reaches a null at $v = 1/NT_r = 1/(8T_r) = 1/T_c$. Note that we denote the cross-ambiguity or delay–Doppler response of a mismatched filter as